

Analysis of a distributed coupling coefficient phase-controlled distributed feedback optical filter

K. Y. Lim, Andy L. Y. Low,^{a)} S. F. Chien, A. H. You, and Y. C. Foo

Faculty of Engineering & Technology, Multimedia University

Jalan Ayer Keroh Lama, 75450 Melaka, Malaysia.

a) andy@mmu.edu.my

Abstract: We have proposed a new phase-controlled distributed feedback wavelength tunable optical filter with distributed coupling coefficient. The analysis, which is based on the transfer matrix method, reveals that an almost constant peak transmissivity (gain) of more than 37 dB, tuning range of better than 21.7 Å and side-mode suppression ratio (SMSR) of more than 17 dB can be achieved using this structure.

Keywords: optical filter, distributed feedback laser diode, distributed coupling coefficient, and transfer matrix method

Classification: Photonics devices, circuits, and systems

References

- [1] S. Suzuki and K. Nagashima, Optical broadband communications network architecture utilizing wavelength-division switching technology, in *Photonic Switching*, T. K. Gustafson and P. W. Smith, Es. Berlin: Springer, pp. 134–137, 1988.
- [2] C. A. Brackett, “Dense wavelength division multiplexing networks: principles and applications,” *IEEE J. Select. Areas Commun.*, vol. 8, pp. 948–964, 1990.
- [3] D. Sadot and E. Boimovich, “Tunable optical filters for dense WDM networks,” *IEEE Commun. Mag.*, pp. 50–55, 1998.
- [4] H. Kogelnik and C. V. Shank, “Coupled-wave theory of distributed-feedback lasers,” *J. Appl. Phys.*, vol. 43, pp. 2327–2335, 1972.
- [5] F. R. Nash, “Mode guidance parallel to the junction plane of double-heterostructure GaAs lasers,” *J. Appl. Phys.*, vol. 44, pp. 4696–4707, 1973.
- [6] T. Numai, “1.5 μm phase-controlled distributed feedback wavelength tunable optical filter,” *IEEE J. Quantum Electron.*, vol. 28, no. 6, pp. 1508–1512, 1992.
- [7] T. Numai, “1.5 μm phase-shift-controlled distributed feedback wavelength tunable optical filter,” *IEEE J. Quantum Electron.*, vol. 28, no. 6, pp. 1513–1519, 1992.

1 Introduction

For realizing large capacity and high-speed information transmission networks, wavelength division multiplexing (WDM), lightwave transmission systems, and wavelength division (WD) photonic switching systems are expected to become the key technologies in realizing broadband communications networks [1, 2]. Wavelength tunable optical filters are key components for WD photonic switching systems in direct detection scheme. A semiconductor wavelength tunable optical filter is basically a laser diode, which is biased slightly below threshold. When an optical signal of a wavelength close to the oscillation wavelength of the device is incident upon the input, the signal is amplified and emitted at the output. By changing the injection current, the wavelength can be tuned due to change in refractive index of the active region. Important optical filter parameters include insertion loss, control mechanism, size, mass-production possibility and low price [3].

In this paper we have analyzed the characteristic performance of a new DFB wavelength tunable filter structure with a passive phase-controlled (PC) waveguide, which is sandwiched between two active sections with distributed coupling coefficient (DCC).

2 Analysis

The analytical model for the filter structure is shown in Fig. 1. This filter consists of a passive phase-controlled waveguide, which is sandwiched between two DFB active sections with distributed coupling coefficient. In this analysis, we have used the transfer matrix method (TMM) to study the characteristics of this filter [4].

The filter cavity is divided into five sections, and a transfer matrix represents the wave propagation in each section. Zero facet reflectivity is assumed, and the z -axis is along the filter cavity. The complex amplitude of the electric

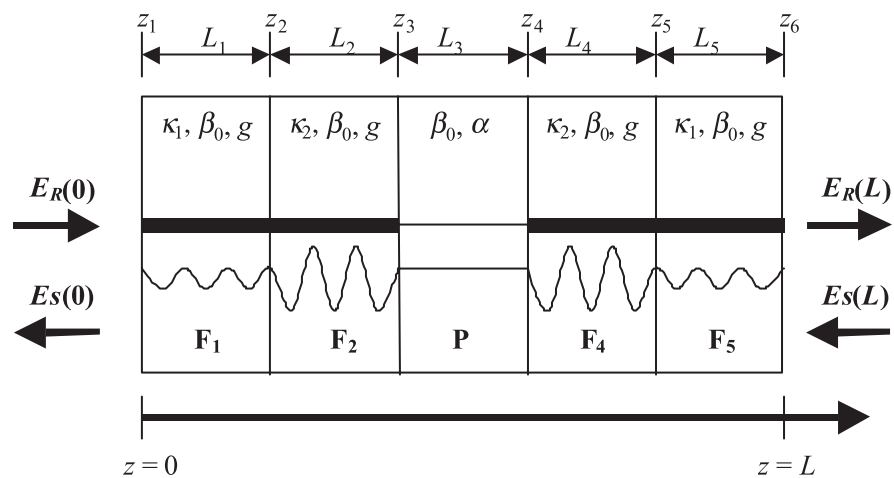


Fig. 1. Analytical model for the phase-controlled DFB with distributed coupling coefficient.

field $E(z)$ inside the filter cavity can be expressed as:

$$\begin{aligned} E(z) &= E_R(z) + E_S(z) \\ &= R(z) \exp(-j\beta_0 z) + S(z) \exp(j\beta_0 z) \end{aligned} \quad (1)$$

where $E_R(z)$ and $E_S(z)$ are the normalized electric fields that propagate along opposite directions, $R(z)$ and $S(z)$ are complex amplitudes of the forward and back ward electric fields, respectively, $\beta_0 = \pi/\Lambda$ is the Bragg frequency of the gratings, and Λ is the grating period.

Substituting Eq. (1) into reduced equations, and neglecting the second derivatives of both $R(z)$ and $S(z)$ with respect to z , as they are slowly varying function of z , we obtained the following pair of coupled-mode equation [4]:

$$\frac{dR(z)}{dz} + (\alpha - j\delta) R(z) = j\kappa S(z) \quad (2a)$$

$$\frac{dS(z)}{dz} + (\alpha - j\delta) S(z) = j\kappa R(z) \quad (2b)$$

In both equations (2a) and (2b), α is the mode gain per unit length, $\delta = \beta - \beta_0$ is the detuning of the propagation constant β from the Bragg propagation constant β_0 , and κ is the grating coupling coefficient. In order to calculate the transmission characteristics of this filter structure, it is more convenient to use TMM where the cavity is divided into five sections. In each section, we assume that parameters α , δ , and κ are uniform. From the coupled-mode equations, the transfer matrix, which describes the propagating electric field in the corrugated section z_i and z_{i+1} ($i = 1, 2, \dots, 5$), can be expressed as

$$\begin{bmatrix} E_R(z_{i+1}) \\ E_S(z_{i+1}) \end{bmatrix} = \begin{bmatrix} f_{11} & f_{12} \\ f_{21} & f_{22} \end{bmatrix} \cdot \begin{bmatrix} E_R(z_i) \\ E_S(z_i) \end{bmatrix} = F_i \begin{bmatrix} E_R(z_i) \\ E_S(z_i) \end{bmatrix} \quad (3)$$

where the matrix elements of matrix F_i are given as follows:

$$f_{11} = \frac{1}{1 - \rho_i^2} \left(E_i - \frac{\rho_i^2}{E_i} \right) \exp[-j\beta_0(z_{i+1} - z_i)] \quad (4a)$$

$$f_{12} = \frac{-\rho_i}{1 - \rho_i^2} \left(E_i - \frac{1}{E_i} \right) \exp[-j\beta_0(z_{i+1} + z_i)] \quad (4b)$$

$$f_{21} = \frac{\rho_i}{1 - \rho_i^2} \left(E_i - \frac{1}{E_i} \right) \exp[j\beta_0(z_{i+1} + z_i)] \quad (4c)$$

$$f_{22} = \frac{1}{1 - \rho_i^2} (E_i - \rho_i^2 E_i) \exp[j\beta_0(z_{i+1} - z_i)] \quad (4d)$$

with

$$E_i = \exp[\gamma_i(z_{i+1} - z_i)] \quad (4e)$$

$$\rho_i = \frac{j\kappa}{\alpha_i - j\delta_i + \gamma_i} \quad (4f)$$

In the above equations, γ_i is the complex propagation constant that satisfies the following dispersion equation:

$$\gamma_i^2 = (\alpha_i - j\delta_i)^2 + \kappa^2 \quad (5)$$

On the other hand, since there is no active section and no grating in the planar PC section (i.e., $\alpha_i = 0$ and $\kappa_i = 0$), the transfer matrix for the electric field of this section is simplified to

$$\begin{bmatrix} E_R(z_{i+1}) \\ E_S(z_{i+1}) \end{bmatrix} = \begin{bmatrix} \exp(\varphi) & 0 \\ 0 & \exp(-\varphi) \end{bmatrix} \cdot \begin{bmatrix} E_R(z_i) \\ E_S(z_i) \end{bmatrix} = P_i \begin{bmatrix} E_R(z_i) \\ E_S(z_i) \end{bmatrix} \quad (6)$$

where $\varphi = (\gamma_p L_p - j\beta_0)$, γ_p is the value of γ_i in the PC section, and L_p is the length of the PC section. The amount of phase shift Ω introduced by the PC section is given by [5]:

$$\Omega = \text{Im}(2\gamma_p L_p) = \frac{4\pi(n_a - n_p)L_p}{\lambda_B} \quad (7)$$

where n_a and n_p are the effective indices of the active and PC sections, respectively. The value of n_p decreases as the current injection into the PC section increases; hence, according to eq. (7), the value of Ω increases.

By multiplying matrices representing the planar phase-controlled sections and the corrugated DFB sections together, the overall transfer matrix for the structure shown in Fig. 1 becomes

$$\begin{aligned} \begin{bmatrix} E_R(L) \\ E_S(L) \end{bmatrix} &= \begin{bmatrix} T_{11} & T_{12} \\ T_{21} & T_{22} \end{bmatrix} \cdot \begin{bmatrix} E_R(0) \\ E_S(0) \end{bmatrix} \\ &= F_5 F_4 P F_2 F_1 \begin{bmatrix} E_R(0) \\ E_S(0) \end{bmatrix} \end{aligned} \quad (8)$$

where $z_1 = 0$ and $z_6 = L = \sum_{i=1}^5 L_i$ are assumed in the above equation. The power transmissivity T in an optical filter is defined as

$$T = \left| \frac{E_S(L)}{E_R(0)} \right|^2 = \left| \frac{1}{T_{22}} \right|^2 \quad (9)$$

The threshold gain α_{th} and the detuning parameter δ can be obtained by solving the following equation numerically:

$$T_{22}(\alpha_{th}, \delta) = 0 \quad (10)$$

The power transmissivity of the filter can be calculated by using the following expression:

$$T = \left| \frac{1}{T_{22}(\alpha = 0.98\alpha_{th}, \delta)} \right|^2 \quad (11)$$

In Eq. (11), we have used $\alpha = 0.98\alpha_{th}$ to achieve a higher output power, and hence a smaller 10 dB bandwidth. Taking into account the longitudinal change of the coupling coefficient and the position of corrugation change in the DCC sections, the coupling ratio (r) and corrugation position (CP) are defined such that:

$$r = \kappa_1 / \kappa_2 \quad (12)$$

$$CP = L_1 / (L_1 + L_2) = L_5 / (L_4 + L_5) \quad (13)$$

where κ_1 and κ_2 are coupling coefficients of the DCC sections

3 Results and Discussions

The total length of the filter cavity $L = 500 \mu\text{m}$ where $L_1 + L_2 = L_4 + L_5 = 200 \mu\text{m}$, and the length of the PC section $L_3 = 100 \mu\text{m}$. In order that results obtained can be compared with a single PSC DFB filter, a parameter known as the averaged coupling coefficient κ_{avg} is introduced in the DCC section such that:

$$\kappa_{avg} = \kappa_1(CP) + \kappa_2(1 - CP) \quad (14)$$

Figure 2 demonstrates the variation of wavelength tuning range of the filter with corrugation position. Results obtained from various coupling coefficient ratios κ_1/κ_2 are compared. It is shown that all curves converge at both $CP = 0$ and $CP = 1$ which corresponds to a 1 PC DFB filter structure with uniform coupling coefficient which was proposed by T. Numai [6]. For a DCC PC DFB filter having $\kappa_1/\kappa_2 < 1$, there is a substantial improvement in the tuning range with the CP value, whereas for the same structure employing $\kappa_1/\kappa_2 > 1$ shows reduced tuning range. Along the curve of $\kappa_1/\kappa_2 = 1/3$, a peak tuning range of 21.7 \AA is found at $CP = 0.4$.

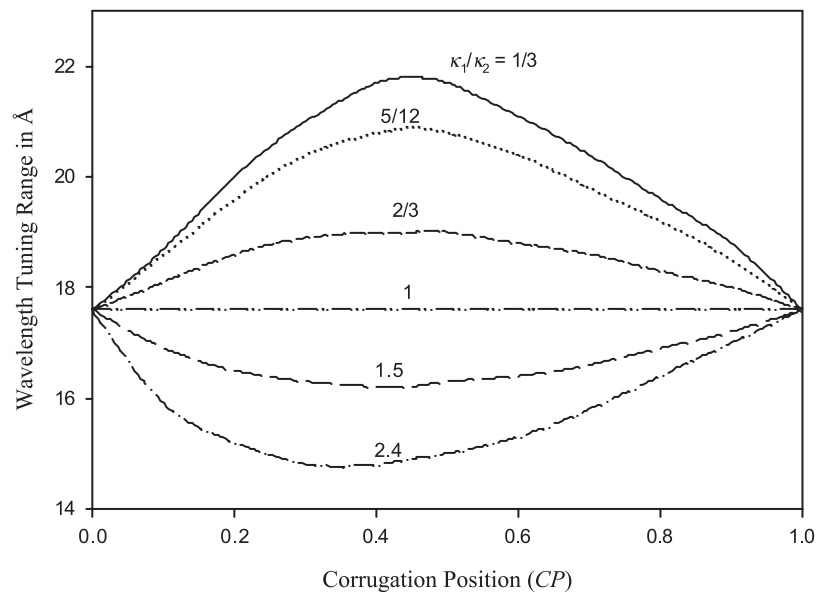


Fig. 2. Variation of the wavelength tuning range versus CP for different coupling ratio. $\kappa_{avg} = 5 \text{ mm}^{-1}$, $\Lambda = 0.21 \mu\text{m}$.

Figure 3 shows the transmission spectrum of the filter for various values of Ω ranging from 0 to 2π . The parameters used in this analysis are $\kappa_1\kappa_2 = 1/3$, $\kappa_{avg} = 5 \text{ mm}^{-1}$, $\Lambda = 0.21 \mu\text{m}$, $CP = 0.4$. The analysis indicates that as the value of Ω increases, the transmissivity peaks exhibit blue shifting (i.e. shift to the negative side of the horizontal axis). The SMSR for the filter varies from 17.3 dB to 29.8 dB, which is above the ITU-T standard of 10 dB. The tuning range of the filter is 21.7 \AA compare with both optical filter structures proposed by T. Numai with only 3.4 \AA and 9.5 \AA tuning range in [6, 7]. The

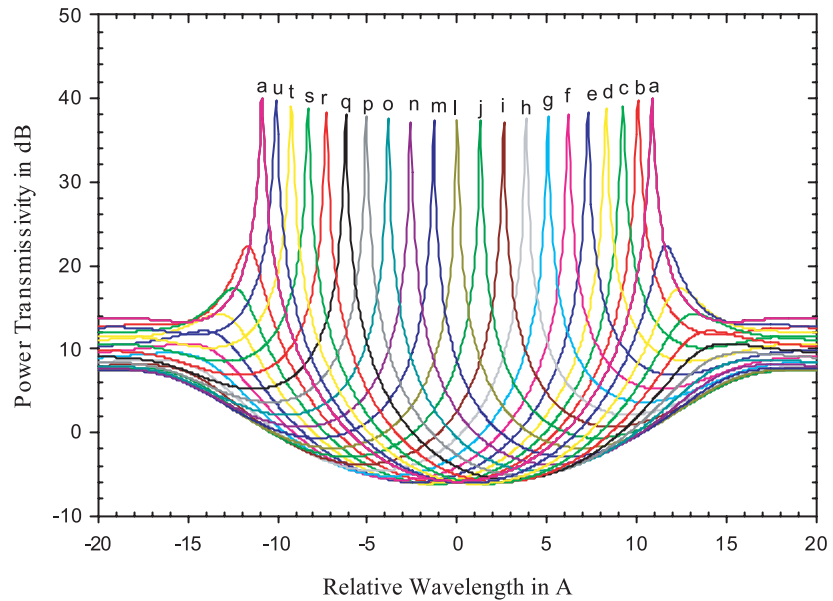


Fig. 3. Power transmissivity versus relative wavelength ($\lambda - \lambda_B$) for different values of Ω . Also $\kappa_{avg} = 5 \text{ mm}^{-1}$, $\Lambda = 0.21 \mu\text{m}$, $\kappa_1/\kappa_2 = 1/3$, $CP = 0.4$ and $L_3 = 100 \mu\text{m}$. Labels a to u represent values of Ω from $0/2.0\pi$ to 1.9π in steps of 0.1π .

peak values of transmissivity within this tuning range are almost constant and ranges from 37.2 to 40 dB (i.e. 2.8 dB deviation).

4 Conclusion

The effects of incorporating DCC with PC DFB filter have been studied. It was found that when $\kappa_1/\kappa_2 < 1$, the filter's tuning range increases, while it decreases for $\kappa_1/\kappa_2 > 1$. An almost constant peak transmissivity (gain) of more than 37 dB, tuning range of better than 21.7 \AA and side-mode suppression ratio (SMSR) of more than 17 dB can be achieved using this structure.